X-ray Probes of ALPs

Francesca Chadha-Day

IPPP, Durham University

Barolo Astroparticle Meeting June 2024

Outline

1. Introduction
2. ALP-Photon Conversion in Galaxy Clusters
3. Magnetic Field Simulation
4. Machine Learning
5. Polarization
6. Conclusions

Galaxy Clusters

- In a background magnetic field, ALPs and photons interconvert.
- Here we consider non-resonant long base line conversion.
- $P \sim B_{\mathrm{perp}}^2 . L . L_{\mathrm{coherence}}$
- Galaxy clusters have $L \sim \mathrm{Mpc}$ and $L_{\mathrm{coherence}} \sim 10\,\mathrm{kpc}$.

ALP-photon conversion

$$\left(\omega + \begin{pmatrix} \Delta_\gamma & 0 & \Delta_{\gamma ax} \\ 0 & \Delta_\gamma & \Delta_{\gamma ay} \\ \Delta_{\gamma ax} & \Delta_{\gamma ay} & \Delta_a \end{pmatrix} - i\partial_z\right) \begin{pmatrix} |\gamma_x\rangle \\ |\gamma_y\rangle \\ |a\rangle \end{pmatrix} = 0$$

- $\Delta_\gamma = \frac{-\omega_{pl}^2}{2\omega}$
- Plasma frequency: $\omega_{pl} = \left(4\pi\alpha\frac{n_e}{m_e}\right)^{\frac{1}{2}}$
- $\Delta_a = \frac{-m_a^2}{\omega}$.
- Mixing: $\Delta_{\gamma ai} = g_{a\gamma}B_i$

$$P_{a\rightarrow\gamma}(L) = |\langle 1,0,0|f(L)\rangle|^2 + |\langle 0,1,0|f(L)\rangle|^2$$

Single domain

$$\tan(2\theta) = \frac{4 g_{a\gamma} B_{\perp} \omega}{\omega_{pl}^2},$$
$$\Delta = \frac{(\omega_{pl}^2 - m_a^2) L}{4\omega}.$$

$$P(a \ \rightarrow \gamma) = \sin^2 (2\theta) \sin^2 \left(\frac{\Delta}{\cos 2\theta} \right)$$

Why X-rays?

- ALP-photon oscillation length $L_{\mathrm{osc}} \sim \frac{4\omega}{\omega_{pl}^2 - m_a^2}$.
- In galaxy clusters, $\omega_{pl} \sim 10^{-12}\,\mathrm{eV}$.
- For $m_a \lesssim 10^{-12}\,\mathrm{eV}$, $L_{\mathrm{osc}} \sim L_{\mathrm{cluster}}$ when $\omega \sim \mathrm{keV}$.

Spectral Modulations

We search for ALPs by studying the X-ray spectra of point sources in or behind galaxy clusters.

Galaxy clusters

Photon-ALP conversion in Galaxy Clusters

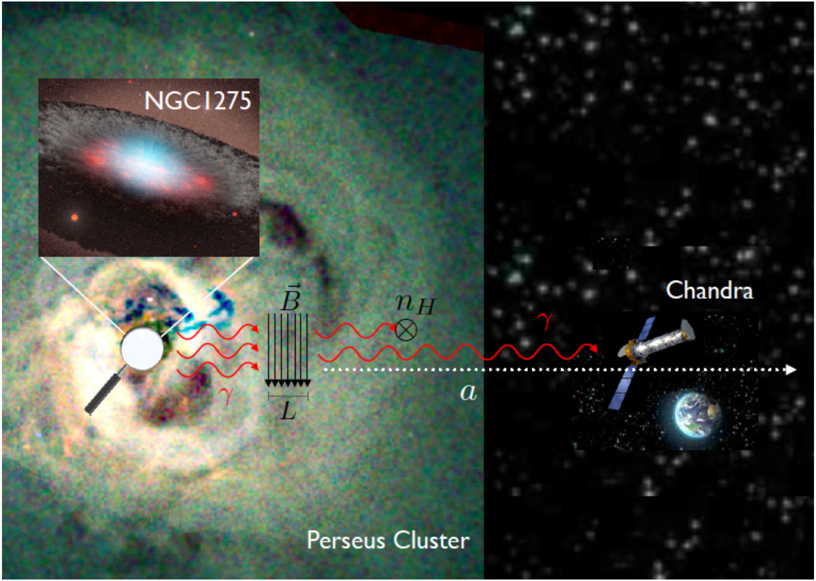

Photon-ALP conversion in Galaxy Clusters

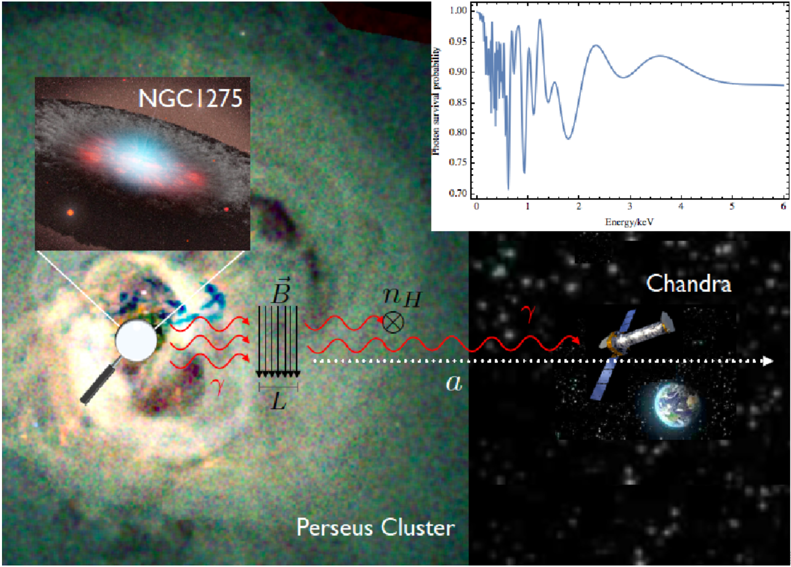

Photon-ALP Conversion

- Photon to ALP conversion can lead to modulations in an initially pure photon spectrum, given by the photon survival probability $P_{\gamma\to\gamma}(E)$.
- At X-ray energies in galaxy clusters, $P_{\gamma\to\gamma}(E)$ is pseudo-sinusoidal in $\frac{1}{E}$.
- ALP induced oscillations in $P_{\gamma\to\gamma}(E)$ would be imprinted on the observed spectrum.
- We seek to constrain $g_{a\gamma}$ by searching for such oscillations.

Photon survival probability

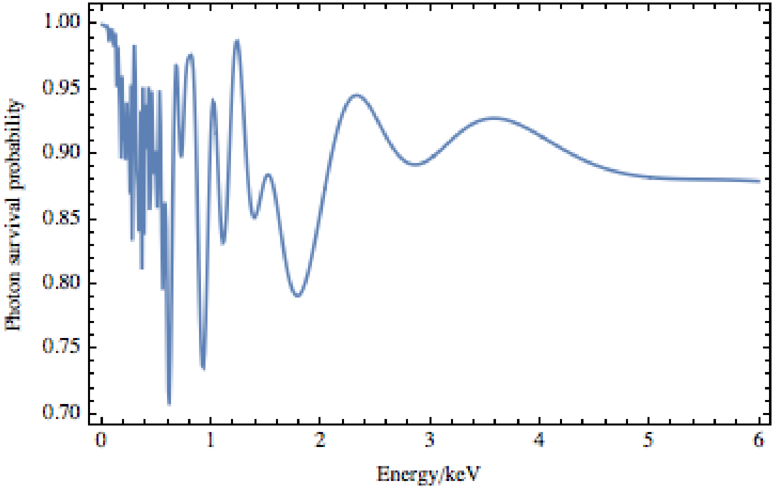

Photon survival probability

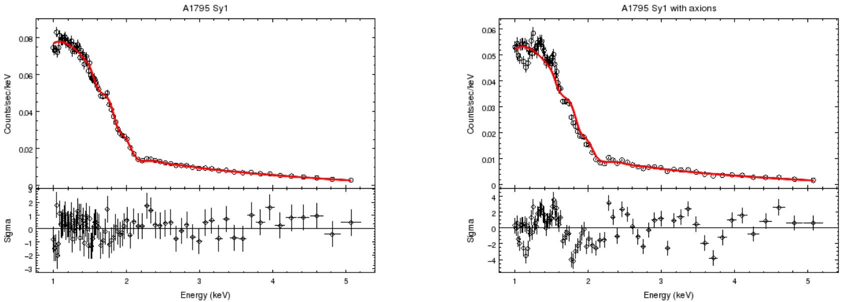

Left: the observed spectrum of the Seyfert galaxy 2E3140 in the galaxy cluster A1795 fitted with an absorbed power law. Right: the same spectrum multiplied by the photon survival probability for a realisation of the A1795 magnetic field and assuming the existence of ALPs with $g_{a\gamma} = 5 \times 10^{-12}\,\mathrm{GeV}^{-1}$.

Bounds

The leading bounds are from *Chandra* transmission grating spectroscopy of quasar H1821+643 (J Sisk-Reynés *et al*, 2109.03261):

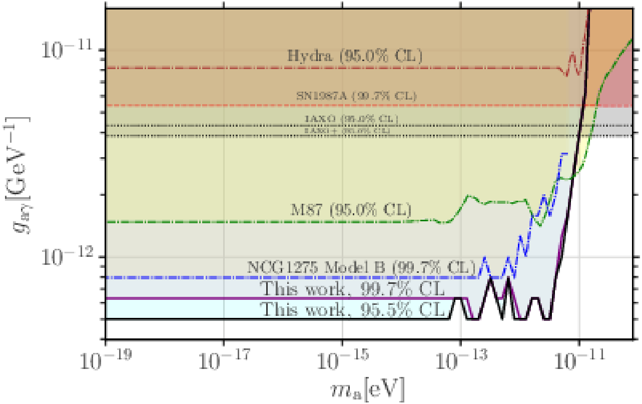

Further improvements

- **Future X-ray telescopes**
  J Conlon *et al*, 1707.00176; J Sisk-Reynés *et al*, 2211.05136

Further improvements

- **Future X-ray telescopes**

  J Conlon *et al*, 1707.00176; J Sisk-Reynés *et al*, 2211.05136
- **Fourier analysis**

  J Conlon & M Rummel, 1808.05916

  MCD Marsh *et al*, 2107.08040

Further improvements

- **Future X-ray telescopes**
  J Conlon *et al*, 1707.00176; J Sisk-Reynés *et al*, 2211.05136
- **Fourier analysis**
  J Conlon & M Rummel, 1808.05916
  MCD Marsh *et al*, 2107.08040
- **Polarization**
  FCD & S Krippendorf, 1801.10557

Further improvements

- **Future X-ray telescopes**

  J Conlon *et al*, 1707.00176; J Sisk-Reynés *et al*, 2211.05136
- **Fourier analysis**

  J Conlon & M Rummel, 1808.05916

  MCD Marsh *et al*, 2107.08040
- **Polarization**

  FCD & S Krippendorf, 1801.10557
- **Machine learning**

  J. Conlon & M. Rummel, 1808.05916

  FCD & S Krippendorf, 1907.07642

  S Schallmoser, S Krippendorf, FCD & J Weller, 2108.04827

  J Sisk-Reynés *et al*, 2211.05136

Further improvements

- **Future X-ray telescopes**

  J Conlon *et al*, 1707.00176; J Sisk-Reynés *et al*, 2211.05136
- **Fourier analysis**

  J Conlon & M Rummel, 1808.05916

  MCD Marsh *et al*, 2107.08040
- **Polarization**

  FCD & S Krippendorf, 1801.10557
- **Machine learning**

  J. Conlon & M. Rummel, 1808.05916

  FCD & S Krippendorf, 1907.07642

  S Schallmoser, S Krippendorf, FCD & J Weller, 2108.04827

  J Sisk-Reynés *et al*, 2211.05136
- **Effect of magnetic field modelling**

  S Schallmoser, S Krippendorf, FCD & J Weller, 2108.04827

  J Matthews *et al*, 2202.08875

Magnetic Fields in Galaxy Clusters

- Determined by Faraday rotation measures
- Can estimate the amplitude and statistical properties of the magnetic field, but not the exact field configuration
- $B(r) \sim B_0 \left(\frac{n_e(r)}{n_0}\right)^{\eta}$
- $n_e(r) = n_0 \left(1 + \frac{r^2}{r_c^2}\right)^{-3\beta/2}$
- Power spectrum within a range of typical coherence lengths $\Lambda_{\mathrm{min}} - \Lambda_{\mathrm{max}}$

1D modelling

- Used by most work
- Simulate only the line of sight to the source
- The magnetic field is modelled by domains of constant field magnitude and direction
- Domain length taken from a distribution of coherence lengths for the cluster
- Magnetic field direction is randomized in in each domain
- Magnetic field is discontinuous and not divergence free

3D modelling

- Start in Fourier space, randomly generating a vector potential with power spectrum $\left|\tilde{A}_k\right|^2 \sim k^{-(n+2)}$ between $k_{\text{min}} = 2\pi/\Lambda_{\text{max}}$ and $k_{\text{max}} = 2\pi/\Lambda_{\text{min}}$
- Magnetic field in Fourier space: $\tilde{\mathbf{B}}(\mathbf{k}) = i\mathbf{k} \times \tilde{\mathbf{A}}(\mathbf{k})$
- Fourier transform $\tilde{\mathbf{B}}(\mathbf{k})$ to obtain a real space field
- The radial distribution of the field amplitude is implemented as a multiplicative factor
- The 3D field is more realistic but takes much longer to generate

Magnetic field comparison

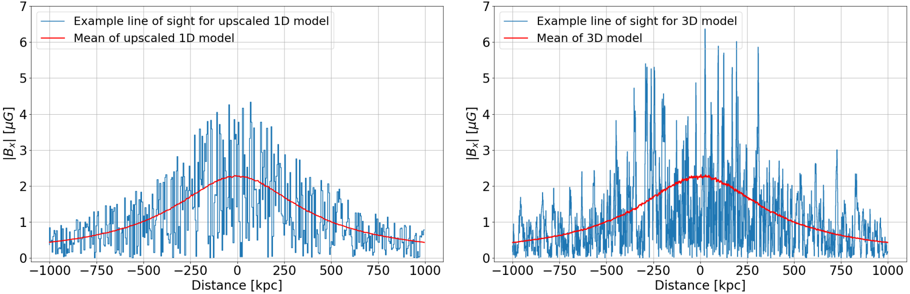

Magnetic field comparison

Bounds using $\chi^2_{\rm red}$ as a test statistic for the source A1795Sy1:

- 1D model (not upscaled): $\mathbf{g_{a\gamma\gamma} \lesssim 1.5 \times 10^{-12}\,GeV^{-1}}$
- 1D model (upscaled): $\mathbf{g_{a\gamma\gamma} \lesssim 1.1 \times 10^{-12}\,GeV^{-1}}$
- 3D model: $\mathbf{g_{a\gamma\gamma} \lesssim 0.9 \times 10^{-12}\,GeV^{-1}}$

Magnetic field comparison

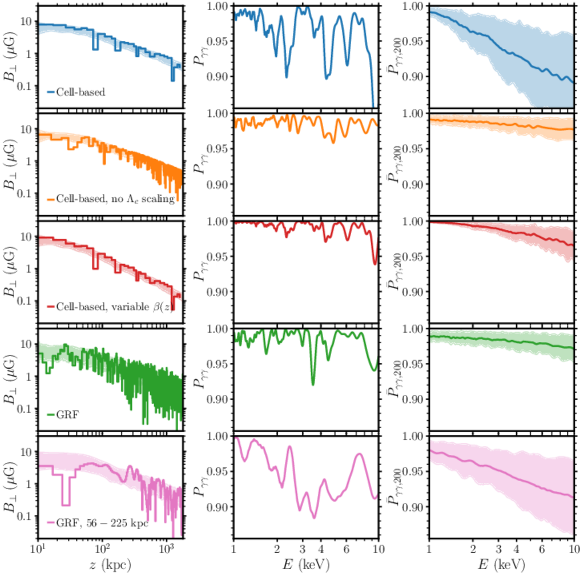

Magnetic field model comparison for Perseus, from J Matthews *et al*, 2202.08875.

Magnetic field comparison

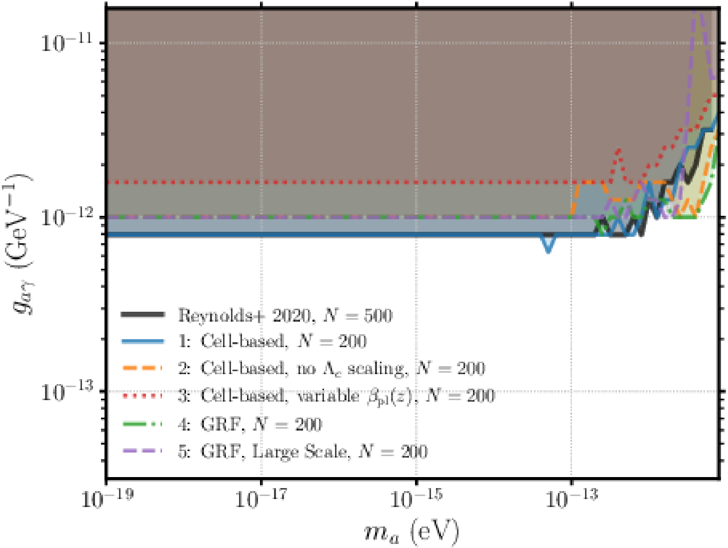

J Matthews *et al*, 2202.08875.

Machine Learning

Seek a function:

$$f(D_i) = \begin{cases} 0, \text{if no ALPs} \\ 1, \text{if ALPs}, \end{cases}$$

based on a training set of examples of each case.

We must use residuals rather than the raw data as the initial amplitude and slope of the source are unknown.

Classifiers

- We train a set of classifiers $\{C_{g_{a\gamma\gamma}}\}$. Classifier $C_{g_{a\gamma\gamma}}$ is trained with fake ALP data *residuals* with coupling $g_{a\gamma\gamma}$. For sufficiently low $g_{a\gamma\gamma}$, the classifier will not be better than random.
- We wish to use these classifiers to place bounds on $g_{a\gamma\gamma}$.
- The ALP-photon interaction $g_{a\gamma\gamma}$ controls the size of the ALP induced effects.

Classifier Performance

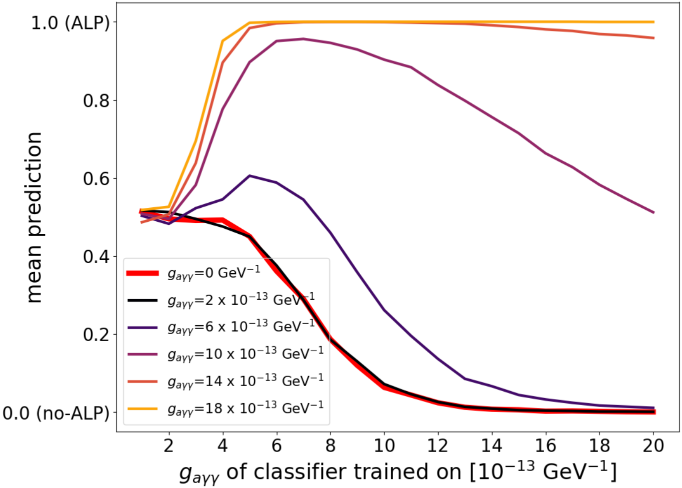

QDA classifier trained with simulated observations of A1795Sy1.

Approximate Bayesian computation

- Used when the likelihood cannot be calculated or would be computationally prohibitive to calculate.
- The posterior distribution is instead *simulated*.
- Review: S Sisson, Y Fan & M Beaumont, 1802.09720

Approximate Bayesian computation

Our summary statistic TS for a data set D_i is the highest $g_{a\gamma\gamma}$ such that $C_{g_{a\gamma\gamma}}$ classifies D_i as containing ALPs.

1. Feed all test sets into all classifiers. Our test sets are evenly space in $g_{a\gamma\gamma}$ i.e. we assume a uniform prior.
2. Calculate the test statistic in each case.
3. If the summary statistic of the test data is the same as for the real data, we *accept* the coupling of the test data.

Approximate Bayesian computation

- As output we obtain a set of $g_{a\gamma\gamma}$ sampled from the posterior distribution which can be used to approximate the posterior.
- Values for $g_{a\gamma\gamma}$ larger than the 95th percentile of the approximated posterior distribution can then be excluded at a 95% confidence level.

Approximate Bayesian computation

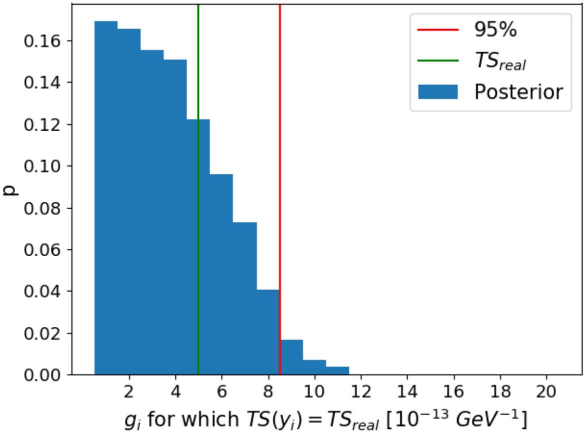

ApBC-approximated posterior distribution and its 95th percentile for the QDA classifiers of the Sy1 galaxy 2E3140 within A1795.

Results: Sy1 2E3140 galaxy within A1795

Method	Bound (GeV^{-1})
χ^2	0.9
Decision Tree Classifier	1.1
AdaBoost Classifier	0.9
Random Forest Classifier	0.9
Gaussian Naive Bayes	0.9
Support Vector Machine	1.4
Quadratic Discriminant Analysis	0.9

Results: Quasar CXOU J134905.8+263752 behind A1795

Method	Bound (GeV^{-1})
χ^2	1.0 (84% C. L.)
Decision Tree Classifier	No bound
AdaBoost Classifier	No bound
Random Forest Classifier	1.9
Gaussian Naive Bayes	No bound
Support Vector Machine	0.6
Quadratic Discriminant Analysis	1.6

Machine learning and Athena

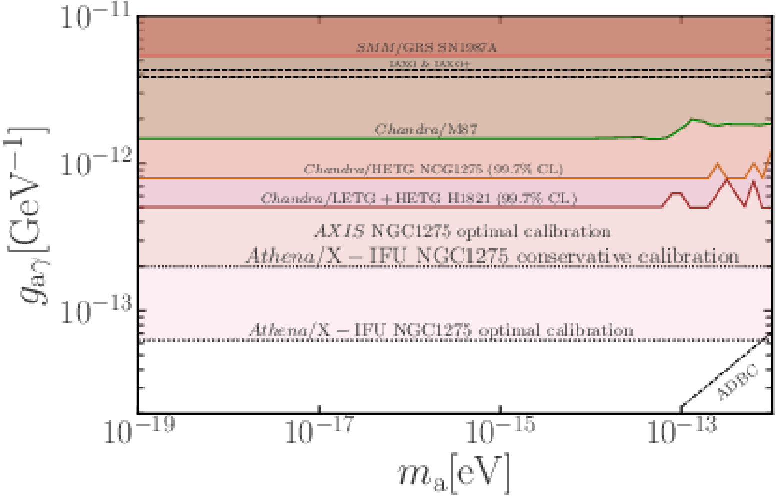

From J Sisk-Reynés *et al.* 2211.05136

ALP-photon conversion

$$\left(\omega + \begin{pmatrix} \Delta_\gamma & 0 & \Delta_{\gamma ax} \\ 0 & \Delta_\gamma & \Delta_{\gamma ay} \\ \Delta_{\gamma ax} & \Delta_{\gamma ay} & \Delta_a \end{pmatrix} - i\partial_z\right) \begin{pmatrix} |\,\gamma_x\rangle \\ |\,\gamma_y\rangle \\ |\,a\rangle \end{pmatrix} = 0$$

Only the photon polarization parallel to the external magnetic field participates in ALP-photon conversion.

IXPE

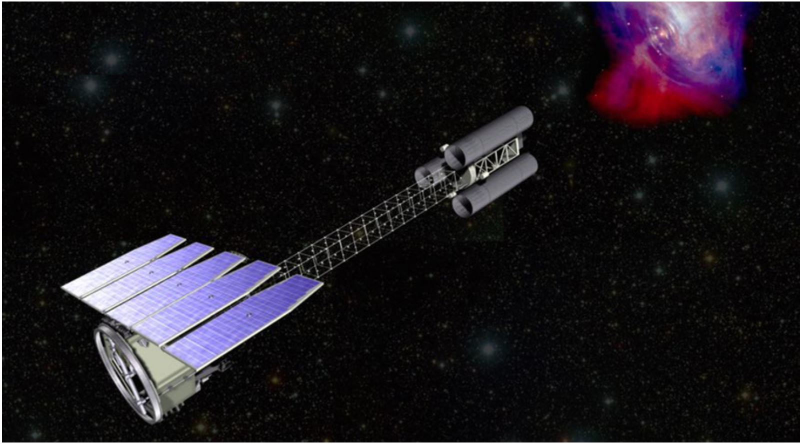

Type I AGN polarization

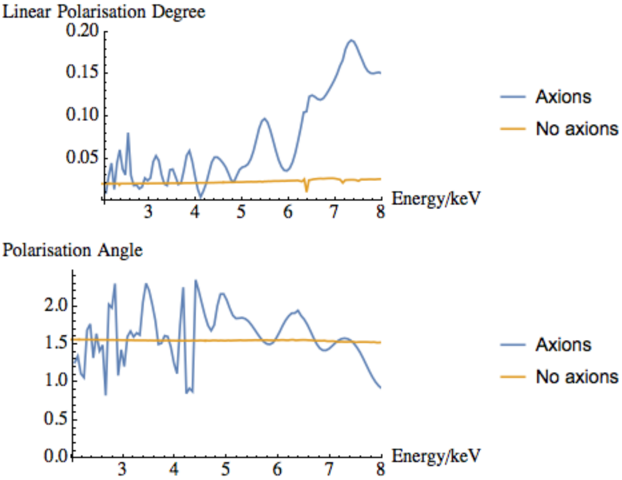

$g_{a\gamma\gamma} = 10^{-12}\,\mathrm{GeV}^{-1}$

Type I AGN polarization

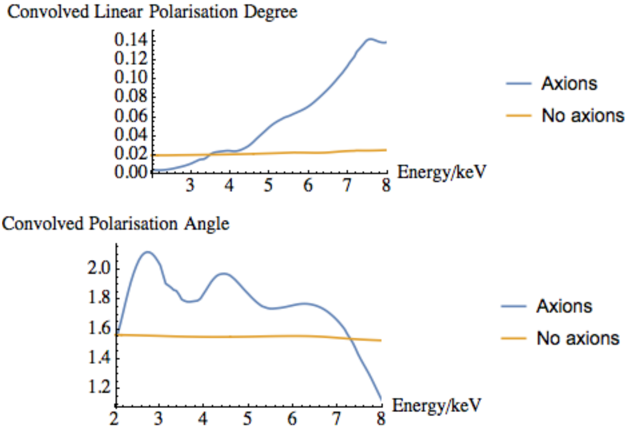

$g_{a\gamma\gamma} = 10^{-12}\,\mathrm{GeV}^{-1}$

Conclusions

- The magnetic fields of galaxy clusters are one of the best ALP to photon converters at low masses.
- Leading bounds on low mass ALPs arise from the observation of point sources shining through galaxy clusters.
- The low hanging fruit in this area has gone, but further improvements are possible.